



ELSEVIER

Physica C 249 (1995) 403–408

PHYSICA C

Coexistence of antiferromagnetic order and superconductivity with T_N higher than T_c in $\text{DyNi}_2\text{B}_2\text{C}$

M.S. Lin ^a, J.H. Shieh ^a, Y.B. You ^a, Y.Y. Hsu ^a, J.W. Chen ^b, S.H. Lin ^c,
Y.D. Yao ^c, Y.Y. Chen ^c, J.C. Ho ^d, H.C. Ku ^{a,*}

^a Department of Physics, National Tsing Hua University, Hsinchu, 300 Taiwan

^b Department of Physics, National Taiwan University, Taipei, 106 Taiwan

^c Institute of Physics, Academia Sinica, Nankang, Taipei, 115 Taiwan

^d Department of Physics and National Institute for Aviation Research, Wichita State University, Wichita, KS 67260, USA

Received 18 April 1995; revised manuscript received 11 May 1995

Abstract

A superconducting transition temperature T_c of 3.8 K with an onset as high as 5.2–5.5 K was reported for quaternary borocarbide $\text{DyNi}_2\text{B}_2\text{C}$ with a high antiferromagnetic Néel temperature T_N around 10.1–10.8 K. No reentrant behavior was observed down to 0.3 K demonstrating a perfect coexistence between superconductivity and antiferromagnetic order. A superconducting upper critical field $H_{c2}(0)$ of 3.0 kG, lower critical field $H_{c1}(0)$ of 200 G and a Ginzburg–Landau parameter κ of 3.7 were derived. A broad T_c transition points to a possible small T_c varying homogeneity range of $\text{DyNi}_{2-\alpha}\text{B}_{2-\beta}\text{C}_{1-\delta}$ in the phase diagram. The magnetic entropy S_m of 10.3 J/mol K or 90% $R\ln 4$ indicates antiferromagnetic ordering of Dy^{3+} with a quadruplet ground state in the tetragonal crystal field. Two field-induced weak-ferromagnetic-like transitions with a field of around 1 T were observed at 2 K.

1. Introduction

Antiferromagnetic ordering which coexists with superconductivity but with a Néel temperature T_N higher than superconducting transition temperature T_c was first observed in the metastable ternary boride HoIr_4B_4 and the related pseudoternary boride systems $\text{R}(\text{Rh}_{1-x}\text{Ir}_x)_4\text{B}_4$ ($\text{R} = \text{Ho}, \text{Dy}$) with composition $x > 0.6$ [1–3]. For example, for the partially Rh substituted $\text{Ho}(\text{Rh}_{0.3}\text{Ir}_{0.7})_4\text{B}_4$ compound, the T_c of 1.6 K observed was below the antiferromagnetic Néel temperature T_N of 2.7 K [2]. For the

$\text{Dy}(\text{Rh}_{0.3}\text{Ir}_{0.7})_4\text{B}_4$ compound, T_c of 1.8 K was below the antiferromagnetic Néel temperature T_N of 4.8 K [3].

Recently, a new magnetic superconductor system was reported in the quaternary borocarbide $\text{RNi}_2\text{B}_2\text{C}$ compounds ($\text{R} = \text{Sc}, \text{Y}, \text{Th}, \text{U}$ or a rare earth) [4–11]. Among many nonmagnetic compounds in the Ni system, $\text{LuNi}_2\text{B}_2\text{C}$ exhibits the highest T_c of 16.6 K [5], followed by 15–16 K for $\text{YNi}_2\text{B}_2\text{C}$ [4,5] and metastable $\text{ScNi}_2\text{B}_2\text{C}$ [7], 8 K for $\text{ThNi}_2\text{B}_2\text{C}$ [9–11] and no superconducting transition was found down to 2 K for $\text{LaNi}_2\text{B}_2\text{C}$ [11]. For compounds containing magnetic rare-earth elements such as $\text{R} = \text{Dy}, \text{Ho}, \text{Er},$ and Tm , lower T_c values were observed due to the magnetic pair-breaking effect [5,8]. A near-

* Corresponding author.

ly reentrant superconductivity was observed for $\text{HoNi}_2\text{B}_2\text{C}$ with $T_c = 8$ K higher than the commensurate T_N of 5.2 K and incommensurate magnetic transition T_m of 6 K [5,8,12–16]. In the magnetic $\text{DyNi}_2\text{B}_2\text{C}$ compound, a superconducting transition temperature $T_{c \text{ onset}}$ around 2 K [8] was reported below the antiferromagnetic-like transition temperature T_N of 10 K, which provides another interesting example with $T_c < T_N$. However, $T_c < 2$ K is too low judging from the variation of T_c in the magnetic $\text{RNi}_2\text{B}_2\text{C}$ compounds [16].

In this work, we have characterized a well-prepared $\text{DyNi}_2\text{B}_2\text{C}$ polycrystalline sample through various experimental techniques including magnetic-susceptibility, magnetic-hysteresis, specific-heat and transport measurements in order to study the interaction and coexistence between superconductivity and magnetic order.

2. Experiments

$\text{DyNi}_2\text{B}_2\text{C}$ samples were prepared from high-purity elements Dy (99.9%, ingot), Ni (99.9% foil), B (99.9995% chips) and C (99.995% chips) with the stoichiometric ratio of (1:2:2:1) under an argon atmosphere in a Zr gettered arc furnace. The Dy, B and C ingredients were wrapped in the Ni foil and arc-melted carefully several times to ensure negligible weight loss and sample homogeneity. The as-melted samples were then wrapped in Ta foils and annealed under argon atmosphere in a sealed quartz tube at 1100°C for 3 days and then quenched in liquid nitrogen. Crystallographic data were obtained with a Rigaku Rotaflex 18 kW rotating anode powder X-ray diffractometer using $\text{Cu K}\alpha$ radiation with a scanning rate of 1° in 2θ per minute. A lazy pulverix-PC program was employed for phase identification and lattice-parameter calculation.

The AC electrical resistivity (16 Hz) measurements were carried out by the standard four-probe method in a dilution refrigerator down to 0.3 K. Magnetic-susceptibility and magnetic-hysteresis measurements were made with a Quantum Design MPMS or a μ -metal shielded MPMS₂ superconducting quantum interference device (SQUID) magnetometer down to 2 K in an applied field from 1 G to 5 T. Low-temperature specific-heat measurements

were made using an adiabatic calorimeter [16] or a relaxation calorimeter [17] from 1.5 K to 20 K.

3. Results and discussion

For three $\text{DyNi}_2\text{B}_2\text{C}$ annealed samples (A, B and C), sample A and C show a minute amount of Ni_2B impurity (<5%) [18]. For sample B, the powder X-ray diffraction pattern as shown in Fig. 1 reflects practically a single phase. The diffraction lines can be well indexed with the $\text{LuNi}_2\text{B}_2\text{C}$ type structure [3] having tetragonal lattice parameters $a = 3.532(3)$ Å, $c = 10.488(5)$ Å and unit-cell volume $V = 130.8(1)$ Å³. A slightly c -axis preferred orientation in the powder pattern was observed judging from the relative intensity of the (004) line as compared with (101) line. The excellent sample quality is attributed to the use of Ni foil as the wrap of the high-purity starting materials, followed by a liquid-nitrogen quench after annealing. Slightly different lattice parameters were observed for other samples ($a = 3.535$ Å, $c = 10.494$ Å and $V = 131.1(1)$ Å³ for sample A; $a = 3.532$ Å, $c = 10.483$ Å and $V = 130.8(1)$ Å³ for sample C) which points to the possibility of a small homogeneity range in the phase diagram with composition $\text{DyNi}_{2-\alpha}\text{B}_{2-\beta}\text{C}_{1-\delta}$.

The low-field (2–3 G), zero-field-cooled (ZFC) DC mass magnetic susceptibilities $\chi_g(T)$ for the annealed bulk samples A, B and C are shown collectively in Fig. 2. An antiferromagnetic-like Néel temperature T_N was observed around 10.2 K. At lower temperature, a sharp superconducting transition tem-

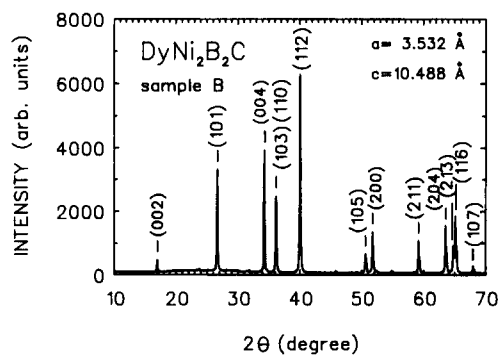


Fig. 1. Powder X-ray diffraction pattern of annealed $\text{DyNi}_2\text{B}_2\text{C}$ sample B.

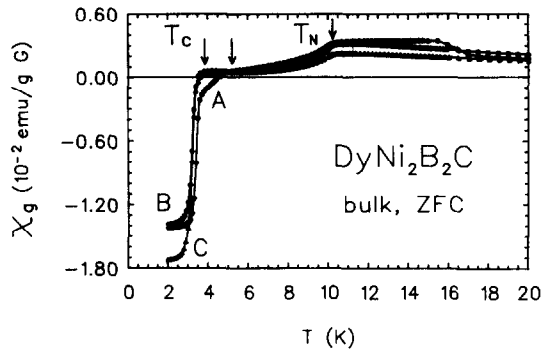


Fig. 2. Temperature dependence of zero-field-cooled (ZFC), low field (2–3 G) mass magnetic susceptibility $\chi_g(T)$ of annealed bulk samples A, B and C.

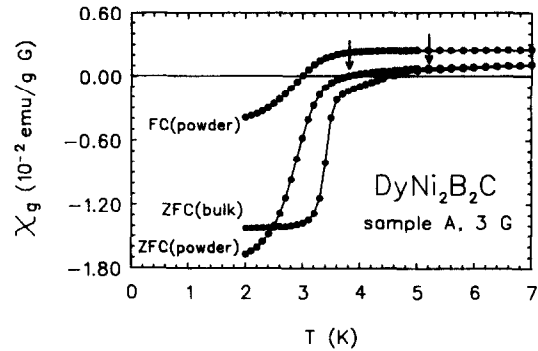


Fig. 3. Low-temperature mass magnetic susceptibility $\chi_g(T)$ of bulk and powder sample A, measured in 3 G field-cooled (FC) and zero-field-cooled (ZFC) modes.

perature T_c of 3.8 K was observed for purer samples B and C. However, a $T_{c \text{ onset}}$ as high as 5.2 K [19] was observed for sample A with an anomalous kink around 16 K not observed for purer samples. All samples show large ZFC signal of $-1.39 \sim -1.72 \times 10^{-2}$ emu/g G at 2 K. Using the X-ray density of 3.982 g/cm^3 for sample B and C, a volume susceptibility percentage $4\pi\chi$ of 70–86% is obtained at 2 K, indicating good bulk superconductivity quality. The antiferromagnetic transition apparently coexists with superconductivity below T_c due to a simple magnetic structure which creates no or a very small internal effective field.

In order to check the T_c broadness and to avoid unwanted superconducting shielding and flux trapping, sample A was powdered to fine particle sizes around $1 \mu\text{m}$ and measured in both zero-field-cooled (ZFC) and field-cooled (FC) mode as shown in Fig. 3. The $T_{c \text{ onset}}$ of 5.2 K is barely visible in the ZFC powder sample which shows a broad transition with diamagnetic onset at 3.8 K. The T_c broadness indicates a possible small homogeneity range with T_c varying composition $\text{DyNi}_{2-\alpha}\text{B}_{2-\beta}\text{C}_{1-\delta}$. In the ZFC mode, Meissner volume susceptibility percentage $4\pi\chi$ at 2 K increases from 71% for bulk sample to 84% for powder sample. For the FC mode, $4\pi\chi$ percentage is reduced to 20% due to flux trapping by defects and impurities during the cooling process. It is noteworthy that the ZFC and FC curves no longer merged at T_c but at the higher T_N .

The low-temperature electrical resistivity $\rho(T)$ for sample C is shown in Fig. 4. A distinct resistivity

drop observed around 10 K is apparently related to the absence of disorder magnetic scattering below the antiferromagnetic transition temperature T_N . A superconducting onset drop around 5.5 K was observed with a $T_{c \text{ midpoint}}$ (50% resistivity drop) transition at 3.8 K and zero resistivity at 3.0 K. No reentrant behavior was observed down to 0.3 K, indicating a perfect coexistence between superconductivity and antiferromagnetic order. The resistivity ratio $\rho(5.5 \text{ K})/\rho(300 \text{ K})$ is 0.045 with a very low residual resistivity $\rho(0 \text{ K})$ of $2.8 \mu\Omega \text{ cm}$ as extrapolated from above T_c . The observed bulk T_c of 3.8 K is indeed very close to the calculated T_c of 3.1 K [16] which can be derived if the magnetic pair-breaking effect is in the framework of the Abrikosov–Gor'kov theory with $\Delta T_c/T_{c0}$ proportional to the de Gennes factor $(g_j - 1)^2 J(J + 1)$, where g_j is the Landé g

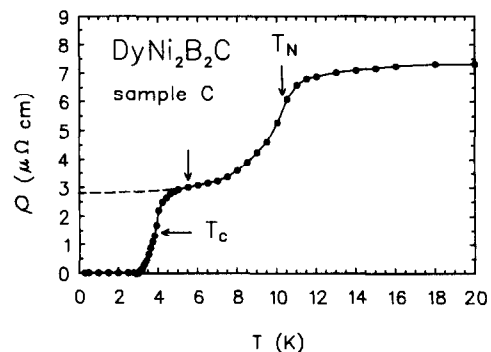


Fig. 4. Low-temperature electrical resistivity $\rho(T)$ of sample C down to 0.3 K.

factor, J is the total angular momentum. The $T_c(\text{Dy})$ of 3.1 K is calculated using $T_{c0}(\text{Dy})$ of 15.3 K as obtained from the variation of T_c with the Ni–Ni in-plane distance $d = a/\sqrt{2}$ (a is the tetragonal lattice parameter) for the nonmagnetic compounds [11,16] at $d = 2.498 \text{ \AA}$ (for $\text{DyNi}_2\text{B}_2\text{C}$ with $a = 3.532 \text{ \AA}$).

The antiferromagnetic transition observed around 10.2 K from magnetic measurements is apparently related to the long-range Dy^{3+} magnetic ordering through the RKKY indirect exchange interaction. The magnetic transition can be clearly corroborated by low-temperature specific-heat data, $C(T)$, for sample C as shown in Fig. 5. A very distinct transition peak was observed at 10.1 K. The expected specific-heat discontinuity at the superconducting transition temperature T_c at 3.8 K would be of the order of mJ/mol K, and is too small to be observed in the presence of a large magnetic contribution. In addition to the small negligible superconducting contribution, there are three contributions to the total heat capacity $C = \gamma T + \beta T^3 + C_m$, corresponding to the electronic, the lattice, and the magnetic transition component, respectively. By employing the literature data for nonmagnetic $\text{LuNi}_2\text{B}_2\text{C}$ [20] as the base line representing the electronic and lattice terms, the magnetic entropy between 1.5 and 20 K can be derived as $S_m = \int [(C - 0.019T - 0.00027T^3)/T] dT = 10.3 \text{ J/mol K}$. Additional contributions to the magnetic entropy below 1.5 K and above 20 K are relatively small judging from the data in Fig. 5.

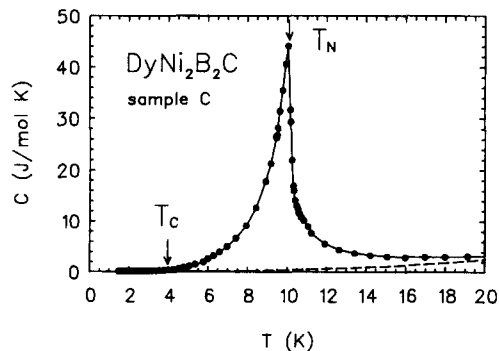


Fig. 5. Low-temperature specific heat $C(T)$ of sample C. The dashed line is the $\gamma T + \beta T^3$ base line from nonmagnetic $\text{LuNi}_2\text{B}_2\text{C}$ above T_c [20].

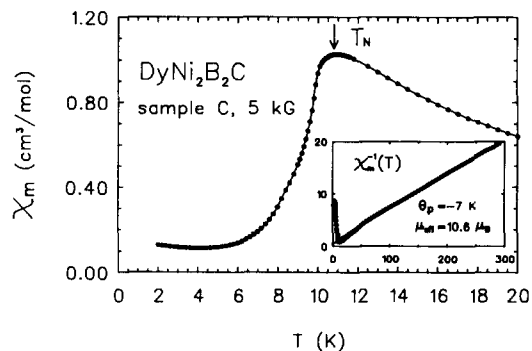


Fig. 6. Temperature dependence of molar magnetic susceptibilities $\chi_m(T)$ and inverse magnetic susceptibility $\chi_m(T)^{-1}$ in a 5 kG field for sample C.

This S_m value of 10.3 J/mol K is close to 90% of $R \ln 4$ and indicates the antiferromagnetic ordering of Dy^{3+} with a possible quadruplet ground state in the tetragonal crystal field.

The molar magnetic susceptibilities $\chi_m(T)$ in the high applied field of 5 kG for sample C is shown in Fig. 6. Superconductivity is completely destroyed in 5 kG, where only the magnetic transition remains with a slightly higher T_N of 10.8 K. A Curie–Weiss behavior was observed above T_N in $\chi_m^{-1}(T)$ as indicated in the inset of Fig. 6, with an effective magnetic moment μ_{eff} of $10.6 \mu_B$ which is very close to the free-ion Dy^{3+} effective moment $g_J[J(J+1)]^{1/2} = 10.63 \mu_B$, and a negative paramagnetic Curie–Weiss intercept θ_p of -7 K which confirms the antiferromagnetic nature of the magnetic order.

Constant-temperature magnetic-hysteresis $M(H)$ measurements provide precise information on the temperature dependence of the superconducting upper critical field $H_{c2}(T)$ and the lower critical field $H_{c1}(T)$. As in Fig. 7, sample B with a sharp T_c at 3.8 K shows a $H_{c2}(T)$ value of 1.75 kG at 2 K as determined from the merging point of the hysteresis curve. Similarly, H_{c2} 's of 1.25 kG at 2.5 K, 750 G at 3 K, 450 G at 3.3 K and 100 G at 3.7 K were obtained. The lower critical field $H_{c1}(T)$ is defined as the deviation from linearity in the initial magnetization in each $M(H)$ curve. The values thus obtained are 100 G at 2 K, 50 G at 2.5 K, 30 G at 3 K and 10 G at 3.3 K. From the temperature dependence of the critical fields, the extrapolated $H_{c2}(0)$ of 3 kG

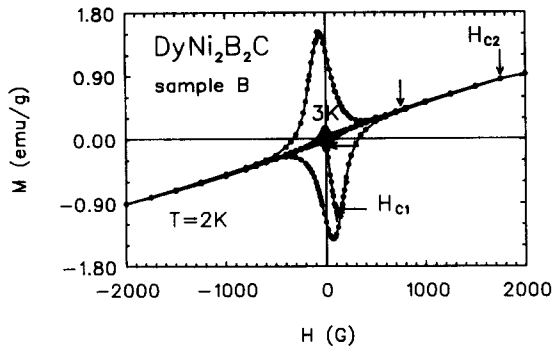


Fig. 7. Intermediate field (up to ± 2 kG) magnetic hysteresis curves $M(H)$ at 2 K and 3 K for sample B. The superconducting upper critical field H_{c2} and lower critical field H_{c1} are indicated by arrows.

and the extrapolated $H_{c1}(0)$ of 200 G are obtained. From $H_{c1}(0)$ and $H_{c2}(0)$, the Ginzburg–Landau parameter κ value of 3.7 is evaluated using the formula $H_{c2}/H_{c1} = 2\kappa^2/(\ln \kappa + 0.5)$ [21]. As a comparison, the κ value of 3.5 is reported for $\text{HoNi}_2\text{B}_2\text{C}$ [16]. The relative low H_{c2} in all quaternary borocarbides [8,16] points to a long coherence length ξ , and three-dimensional-like superconductivity. However, a slightly anisotropic $H_{c2}(T)$ and $H_{c1}(T)$ is still possible due to the field- and orientation-dependent antiferromagnetic ordering which coexist with superconductivity.

Since each $M(H)$ curve has a slightly nonlinear background due to the field dependence of the antiferromagnetic order. A high field $M(H)$ up to 5 T is measured for sample B at 2 K. As shown in Fig. 7,

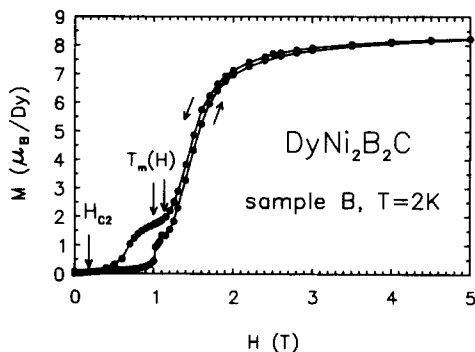


Fig. 8. High-field (up to 5 T) magnetic-hysteresis curve $M(H)$ at 2 K for sample B.

above $H_{c2}(2\text{ K})$ of 1.75 kG, a field-induced weak-ferromagnetic-like transition was observed at 1 T field and a second possible transition around 1.15 T. The ferromagnetic hysteresis curve can easily be detected for these transitions. Similar field-induced magnetic transitions were also observed for $\text{HoNi}_2\text{B}_2\text{C}$ [12,22]. A saturated magnetic moment of $8.3\mu_B$ per Dy is achieved in 5 T field at 2 K, which is already very close to the calculated free-ion $\text{Dy}^{3+}g_JJ = 10\mu_B$ magnetic moment.

$\text{DyNi}_2\text{B}_2\text{C}$ with an antiferromagnetic transition T_N above T_c is indeed very similar to the previous reported $\text{R}(\text{Rh}_{1-x}\text{Ir}_x)_4\text{B}_4$ systems ($\text{R} = \text{Ho}, \text{Dy}$) [1–3], where $T_N > T_c$ were observed for the higher Ir concentration of $x > 0.6$. For the lower Ir concentration region of $0.2 < x < 0.6$, $T_N < T_c$ was observed with a more complex magnetic structure variation. Both regions show coexistence between superconductivity and antiferromagnetic order with no reentrant behavior [1–3,23]. True reentrant behavior can be observed only with the very low Ir concentration of $x < 0.2$. For example, the superconductivity of 5.2 K in $\text{Ho}(\text{Rh}_{0.85}\text{Ir}_{0.15})_4\text{B}_4$ was completely destroyed by a ferromagnetic ordering at the Curie temperature T_C of 2.77 K [2,23]. Since no reentrant behavior was observed for $\text{DyNi}_2\text{B}_2\text{C}$ down to 0.3 K, the antiferromagnetic structure is likely to be a simple commensurate magnetic structure similar to the reported antiferromagnetic structure for $\text{HoNi}_2\text{B}_2\text{C}$ below T_N of 5.2 K [13,14].

4. Conclusions

Well-prepared $\text{DyNi}_2\text{B}_2\text{C}$ samples were characterized by various experimental techniques including magnetic-susceptibility, magnetic-hysteresis, specific-heat and electrical-resistivity measurements. The results yield two distinct phase transitions: a superconducting transition temperature T_c of 3.8 K (with an onset as high as 5.2–5.5 K) and an antiferromagnetic Néel temperature T_N of 10.1–10.8 K. No reentrant behavior was observed down to 0.3 K, indicating a perfect coexistence between superconductivity and antiferromagnetic order. A broad T_c transition points to a possible small T_c varying homogeneity range of $\text{DyNi}_{2-\alpha}\text{B}_{2-\beta}\text{C}_{1-\delta}$ in the phase diagram.

Acknowledgements

This work was supported by the National Science Council of Taiwan under Contract NSC84-2112-M007-003 and -038.

References

- [1] H.C. Ku, B.T. Matthias and H. Barz, *Solid State Commun.* 32 (1979) 937.
- [2] H.C. Ku, F. Acker and B.T. Matthias, *Phys. Lett.* 76 A (1980) 399.
- [3] H.C. Ku and F. Acker, *Solid State Commun.* 35 (1980) 937.
- [4] R. Nagarajan, C. Mazumdar, Z. Hossain, S.K. Dhar, K.V. Gopalakrishnan, L.C. Gupta, C. Godart, B.D. Padalia and R. Vijayaraghavan, *Phys. Rev. Lett.* 72 (1994) 274.
- [5] R.J. Cava, H. Takagi, H.W. Zandbergen, J.J. Krajewski, W.F. Peck Jr., T. Siegrist, B. Batlogg, R.B. van Dover, R.J. Felder, K. Mizuhashi, J.O. Lee, H. Eisaki and S. Uchida, *Nature (London)* 367 (1994) 252.
- [6] T. Siegrist, H.W. Zandbergen, R.J. Cava, J.J. Krajewski and W.F. Peck Jr., *Nature (London)* 367 (1994) 254.
- [7] H.C. Ku, C.C. Lai, Y.B. You, J.H. Shieh and W.Y. Guan, *Phys. Rev. B* 50 (1994) 351.
- [8] H. Eisaki, H. Takagi, R.J. Cava, B. Batlogg, J.J. Krajewski, W.F. Peck Jr., K. Mizuhashi, J.O. Lee and S. Uchida, *Phys. Rev. B* 50 (1994) 647.
- [9] J.L. Sarrao, M.C. de Andrade, J. Herrmann, S.H. Han, Z. Fisk, M.B. Maple and R.J. Cava, *Physica C* 229 (1994) 65.
- [10] T. Takabatake, Y. Maeda, T. Konishi and H. Fujii, *J. Phys. Soc. Jpn.* 63 (1994) 2853.
- [11] C.C. Lai, M.S. Lin, Y.B. You and H.C. Ku, *Phys. Rev. B* 51 (1995) 420.
- [12] P.C. Canfield, B.K. Cho, D.C. Johnston, D.K. Finnemore and M.F. Handley, *Physica C* 230 (1994) 397.
- [13] T.E. Grigereit, J.W. Lynn, Q. Huang, A. Santoro, R.J. Cava, J.J. Krajewski and W.F. Peck Jr., *Phys. Rev. Lett.* 73 (1994) 2756.
- [14] A.I. Goldman, C. Strassis, P.C. Canfield, J. Zarestky, P. Dervenagas, B.K. Cho, D.C. Johnston and B. Sternlieb, *Phys. Rev. B* 50 (1994) 9668.
- [15] H. Schmidt and H.F. Braun, *Physica C* 229 (1994) 315.
- [16] M.S. Lin, J.H. Shieh, Y.B. You, W.Y. Guan, H.C. Ku, H.D. Yang and J.C. Ho, *Phys. Rev. B* (1995), to be published.
- [17] P.J. Jiang, M.S. Lin, J.H. Shieh, Y.B. You, H.C. Ku and J.C. Ho, *Phys. Rev. B* (1995), to be published.
- [18] E.E. Havinga, H. Samasma and P. Hokkeling, *J. Less-Common Met.* 27 (1972) 169 and 281. No superconducting transition down to 0.07 K was reported for the Ni₂B phase.
- [19] B.K. Cho, P.C. Canfield and D.C. Johnston, preprint. A similar $T_{c\text{ onset}}$ around 6 K was reported.
- [20] S.A. Carter, B. Batlogg, R.J. Cava, J.J. Krajewski, W.F. Peck Jr. and H. Takagi, *Phys. Rev. B* 50 (1994) 4216.
- [21] C.R. Hu, *Phys. Rev. B* 6 (1972) 1756.
- [22] M.S. Lin and H.C. Ku, unpublished results.
- [23] K.N. Yang, S.E. Lambert, H.C. Hamaker, M.B. Maple, H.A. Mook and H.C. Ku, *Superconductivity in d- and f-Band Metals*, eds. W. Buckel and W. Weber (Kernforschungszentrum Karlsruhe, 1982) p. 27.